

Light Properties Improvement of Light Emitting Woven Textiles with Optical Fibres for Photodynamic Therapy

Yesim Oguz^{1,2}, Cedric Cochrane^{1,2}, Vladan Koncar^{1,2} and Serge Mordon^{1,3}

¹University Lille Nord de France, F-59000 Lille, France

²ENSAIT, GEMTEX, F-59100 Roubaix, France

³INSERM 1189 ONCO-THAI, Lille University Hospital, CHRU, Lille, France

Keywords: Light Emitting Fabric (LEF), Plastic Optical Fibres (POF), Photodynamic Therapy (PDT), Doehlert Experimental Design, Response Surface Method (RSM).

Abstract: For an efficient and less painful photodynamic therapy (PDT), a light emitting fabric (LEF) was woven from plastic optical fibres (POF) aiming at the treatment of dermatologic diseases such as Actinic Keratosis (AK). The traditional PDT treatments applied with external light sources deliver a non-uniform light distribution on the skin surface due to the anatomical particularity of the human body (head vertex, hand, etc.). Therefore a successful PDT obligates a homogenous and reproducible light delivery. With this purpose, plastic optical fibres (POF) have been woven in textile in order to create macro-bendings and thus emit out the injected light directly to the skin. To improve the light intensity and light emitting homogeneity of the LEF, Doehlert Experimental Design is applied. Fifteen experiments performed to analyze the response surface. Light properties of the prototypes were evaluated. The proposed models fitted well with the experimental data and enabled the optimal set up the warp yarns tensions. This study showed that RSM was a suitable tool to optimize the models of light diffusion properties.

1 INTRODUCTION

Photodynamic therapy (PDT) is a treatment procedure for localized cancer or pre-cancer that requires photosensitizer, tumour oxygenation, and controlled light delivery to provide a treatment efficient (Mordon et al. 2015). Actinic Keratosis, a pre-cancerous skin disease, could be treated via PDT with good cosmetic results.

The traditional PDT modality with external light sources delivers a non-uniform light distribution on the skin surface due to the irregularly shaped cavities or surfaces of the human body (head vertex, hand, etc.) (Mordon, Cochrane, et al. 2015; Cochrane et al. 2011; Cochrane et al. 2013). Therefore, a flexible medical textile was developed for an adequate and homogenous light coverage of the entire tumour with the aim of efficient, reliable and less painful photodynamic therapy for AK treatment.

In this work, a light emitting fabric (LEF) has been woven by inserting POF in weft and Polyester yarns in warp direction. An optimal weaving process has been set up to predetermine macro-bendings of

the POFs, which introduce side emission of light when the critical angle is exceeded. By modifying the weave pattern or modifying the tension on the warp yarns, it is possible to control the macro-bendings of POF, so their side emitting property as a result of weaving process.

A special pattern based on three different satin weaves has been developed to obtain a good homogeneity of light emission and regulate the loss of side emitted radiation intensity along POFs. Furthermore, Doehlert experimental design is applied for developing a statistical model to achieve response surfaces of the effects of the weaving parameters on the light properties of LEF. First, fifteen samples were produced with different tensions on the warp beams calculated by experimental design to find the optimal tension for a good light distribution homogeneity and light intensity of the LEF.

This research work aims at the investigation of the effects of weaving process, as different warp yarn tensions, on the light properties of the LEF. To avoid the high number of experiments and costs with the traditional one time method, the optimization of

the model performed with the most related technic, response surface methodology (RSM).

2 EXPERIMENTAL

2.1 Weaving Process

In this work weaving process was used to create macrobends on the optical fibres to emit the injected light. Optical fibres confine light in the fibre core by its nature, but bending the optical fibre changes the incident angle of the injected light, thus radiative losses occur (see Figure 1). It is possible to modify the radius of macro-bendings, so the bending losses by changing the tension on the warp yarns even if there are other influent factors (textile yarns, weft and warp density, number of turns etc.) on the side-emitting properties (Wang et al. 2013; Lee et al. 2009). Adding tension on warp yarns render them more rigid that effects sharpness of optical fiber macrobends.

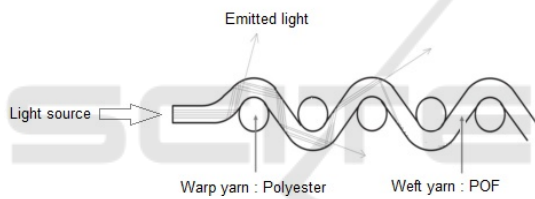


Figure 1: Inserted POF into a textile structure with the weaving process.

Different weaving patterns were woven to see their light intensity decay, and then a special repeating pattern was designed to obtain homogeneous light emission. This specific repeating pattern was a composition of three different satin weaves (SW) and divided in 5 woven areas. Different zones signify the longitudinal bands with same weaving patterns; zone A contains the first and the fifth woven areas, zone B contains the second and the fourth woven areas and zone C contains the third woven area. Figure 2 shows the weaving system with three warp beams that supply the zone A, B and C on the LEF.

The sample size is chosen 200mm width because of the morphology and the overall size of the faces.

2.2 Measurement of Light Intensity and Light Emission Homogeneity

Light intensity and light delivery homogeneity of the LEF samples were measured with a powermeter

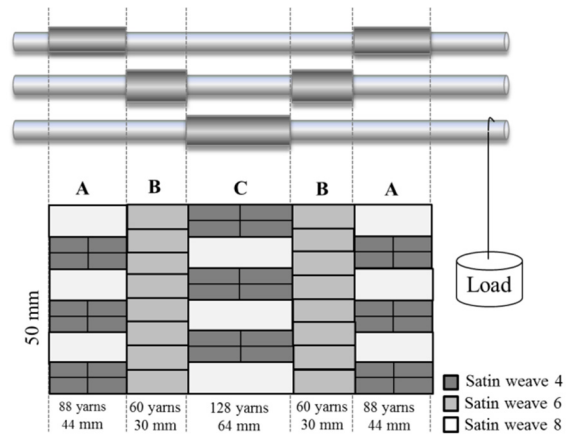


Figure 2: Schema of the warp beams disposition and the designed repeating weave pattern.

(Ophir II, 638nm) while they are connected to lasers (1W) by their two ends (Figure 3). In a dark room, the light intensity power was measured on each cm^2 by excluding the measures 0,5 cm from the borders and 1 cm from the ends.

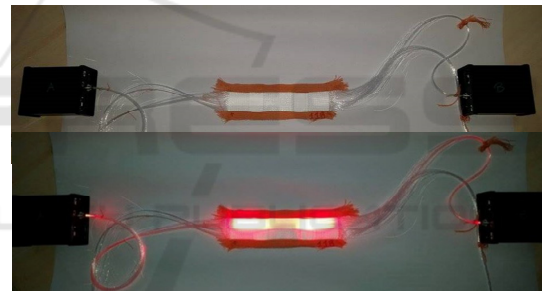


Figure 3: Light emitting fabrics connected to laser by two ends.

Two mathematical formulas were used to reduce the number of values to compare the samples among them. The average of the power per cm^2 , and sum of square deviations of power per cm^2 divided to square of power average were chosen for light intensity (P) and light emission homogeneity (H), respectively. A puissant LEF with homogenous light distribution necessitates a great P value and an H value close to zero.

Furthermore, to avoid the reinjection in the light sources, low light output from the brass boxes is requested. Otherwise reinjection can increase the temperature of the sources and cause device damage. It was also observed that when the LEF was connected to the laser from one side, if the light output from the other end (connector) was low, light intensity of the LEF was high.

2.3 Doehlert Experimental Design

Doehlert design was used to optimize the light intensity and the homogeneity of the LEF woven with optical fibres. The flexibility of the design allows adding new points to explore more the domain without losing quality of the model (Bezerra et al. 2008; Fauduet et al. 2003; Lee & Hamid 2015). The most influential factors on the responses were chosen and studied at 3, 5 and 7 levels: A signifies the added tension on the first zone, B for the second, and C for the third zone (Figure 4). The critical points (minimum, centre, maximum point) were chosen 40, 70, 100 g/warp yarn respectively.

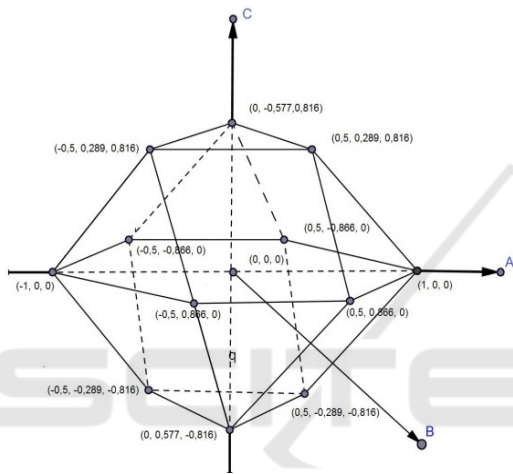


Figure 4: 3D view of the experimental domain. Axis A, B and C are the coded units of the experimental factors.

The general quadratic model with n factors and an experimental response (Y) is given below:

$$Y = b_0 + \sum_{i=1}^n b_i x_i + \sum_{i < j} b_{ij} x_i x_j + \sum_{i=1}^n b_{ii} x_i^2 \quad (1)$$

For a process concerning three factors; Tension of zone 1 (A), Tension of zone 2 (B) and Tension of zone 3 (C), the model is described as:

$$P = p_0 + p_1 A + p_2 B + p_3 C + p_{12} AB + p_{13} AC + p_{23} BC + p_{11} A^2 + p_{22} B^2 + p_{33} C^2 \quad (2)$$

Where, P is predicted response for the average of LEF's light intensity (mW/cm²), A, B, C are independent variables, p₀ is independent term, p₁, p₂, p₃ are the coefficients of the linear terms, p₁₁, p₂₂, p₃₃ are the coefficients of the squared terms and p₁₂, p₂₃, p₁₃ are interaction terms.

The same equation is also used to find the predicted response H for the light emission homogeneity of the LEF, sum of squares of light

puissance deviations divided by the square of puissance average, with the same independent variables A, B, C.

$$H = h_0 + h_1 A + h_2 B + h_3 C + h_{12} A B + h_{13} A C + h_{23} B C + h_{11} A^2 + h_{22} B^2 + h_{33} C^2 \quad (3)$$

3 RESULTS

First of all, fifteen flexible LEFs were produced with the calculated tension settings in order to predict the responses of the light intensity and the light delivery homogeneity of the LEF. The calculated and the experimental responses are given in the table for the quadratic model. The experiments were performed in random order, and the central point (0, 0, 0) experiments were repeated three times to observe test repeatability. Then five more samples were calculated and produced to find the sample with optimal results (see the values on table 1).

The only sample, which has provided the compromise of the expected properties, was sample 15 among the twenty samples of experimental design. The calculated results with the experimental design were achieved with the experiments. Figure 5 shows the light diffusion per cm² for sample 15.

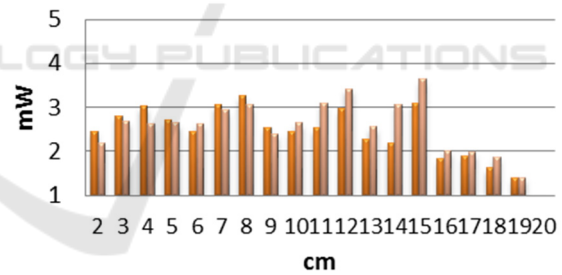


Figure 5: Light emission of sample 15.

Furthermore the analysis of the variance (ANOVA) used to verify the fit of the model; p-value must be compared to chosen significant level (usually α=0,05). If the p-value is less than or equal to α, it means the model terms are highly significant. Otherwise the null hypothesis is accepted. Table 2 demonstrates the model of P has statistically significant terms.

The following equation 4 and equation 5 were found by applying multiple regression analysis on the experimental data. A, B, C correspond to independent variables of two models.

$$\begin{aligned}
 \mathbf{P} = & 2,20 + (-0,32*A) + (0,02*B) + (0,17*C) \\
 & + (-0,05*AB) + (-0,02*AC) + (0,32*BC) \\
 & + (-0,22*A^2) + (0,08*B^2) + (-0,41*C^2)
 \end{aligned}
 \tag{4}$$

$$\begin{aligned}
 \mathbf{H} = & 14,45 + (8,20*A) + (2,12*B) \\
 & + (-4,20*C) + (-5,75*AB) + (-3,72*AC) \\
 & + (-1,91*BC) + (8,01*A^2) + (1,52*B^2) \\
 & + (-3,32*C^2)
 \end{aligned}
 \tag{5}$$

Table 1: Three-factors Doehlert experimental design, with the relative responses.

Experiment	Predicted Results			Experimental Results			
	A	B	C	P	H	P	H
1.1	0	0	0	2,15	15,61	2,11	12,74
1.2	0	0	0	2,15	15,61	2,28	19,96
1.3	0	0	0	2,15	15,61	2,06	14,12
1.4	0	0	0	2,20	14,45	2,55	13,7
2	1	0	0	1,65	30,66	1,65	31,18
3	-1	0	0	2,30	14,26	2,28	15,06
4	0,5	0,866	0	2,05	21,04	1,97	24,77
5	-0,5	-0,866	0	2,41	9,17	2,27	3,59
6	0,5	-0,866	0	2,04	22,35	1,98	21,38
7	-0,5	0,866	0	2,32	17,82	2,39	18,13
8	0,5	0,289	0,816	1,94	12,85	1,92	7,68
9	-0,5	-0,289	-0,816	2,00	10,28	1,82	13,63
10	0,5	-0,289	-0,816	1,64	23,18	1,71	23,32
11	0	0,577	-0,816	1,65	18,30	1,67	13,78
12	-0,5	0,289	0,816	2,23	9,35	2,17	8,66
13	0	-0,577	0,816	1,95	8,99	2,03	14,47
14	-1	-1	-1	2,21	3,16	2,23	5,0
15	-1	-1	-0,6	2,41	5,86	2,43	3,0
16	-1	-1	-0,7	2,37	5,29	2,44	3,8
17	-1	-1,3	-0,6	2,56	4,04	2,57	6,4

Table 2: ANOVA table for the light intensity and the light delivery homogeneity models.

%	Puissance (P)					Homogeneity (H)				
	D	SS	MS	F-	Probability	D	SS	MS	F-value	Probability
Total	20					20				
Constant	1					1				
Total	19	1,52				19	1146,38			
Regression	9	1,28	0,14	5,871	0,005*	9	957,29	106,37	5,625	0,006*
Residual	10	0,24	0,02			10	189,097	18,91		

*Significant at *probability value* ≤ 0,05,
 DF: Degrees of Freedom, SS: Sum of squares, MS: Mean Squares

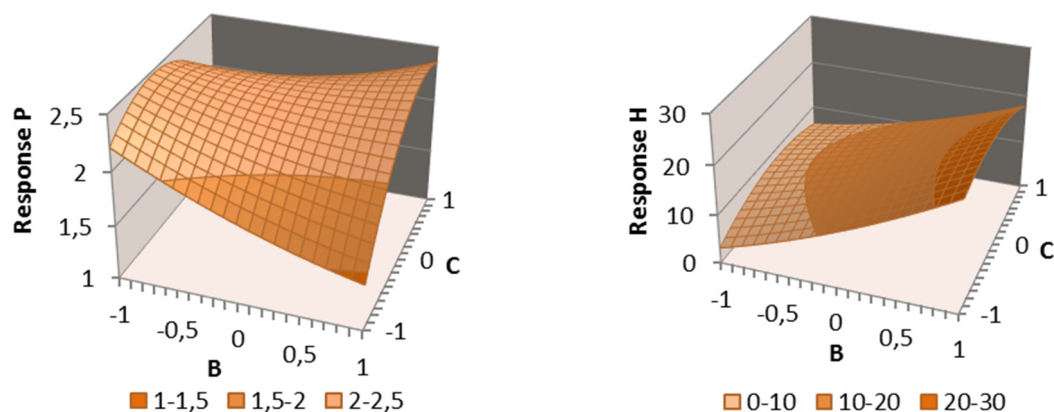


Figure 6: Response surface methodology graphics for the light diffusion models.

Response Surface Methodology (RSM) was used to optimize the modelling for the light emission properties of the LEF. Figure 6 presents the three-dimensional RSM graphics for the light intensity (on the left) and light diffusion homogeneity (on the right) responses of the LEF.

The effects of factors were demonstrated that optimal responses of model P and H could be achieved if A is at its low level. As a result, when A is fixed at its low level; the optimum compromise result for two models is located between -0,4 and -1 (B axis), and between -0,5 and -1 (C axis), while B is not an influential for the P model as obtained with the sample 15.

4 CONCLUSIONS

The present study reports the application of the RSM using the Doehlert experimental design of experiments to develop a mathematical correlation between the tension on the warp yarns and the light diffusion properties of the fabric diffuser.

According to the experimental results of twenty samples, two models were designed with Doehlert matrix. The results proved that the optimum trial in the domain was produced with sample 15, which showed an average light intensity around 2,5 mW and uniform light distribution. Furthermore, the RSM graphs have given more information on the optimal samples. It is certain that the tension of first zone was expected to be at its low level (40g/warp yarn) for the compromise result and there is an important correlation among the tension of zone A, B, C.

Predicted values correspond to the experimental values of the light intensity model, with an experimental error of the same order as that found in

the experimental design. So the model has been a powerful tool for optimizing the light intensity of designed fabric, but it was less suitable for optimizing the light emission homogeneity. This design also allowed us to find the optimal tension settings in few experiences, which was time consuming and inexpensive.

ACKNOWLEDGEMENTS

This work was supported by the GEMTEX Laboratory, European Commission grant PHOSISTOS in the Framework Programme 7, and INSERM for the development and test of a light emitting textile for the treatment of skin disease actinic keratosis.

REFERENCES

- Bezerra, M. A. et al., 2008. Response surface methodology (RSM) as a tool for optimization in analytical chemistry. *Talanta*, 76, pp.965–977.
- Cochrane, C. et al., 2011. Flexible displays for smart clothing : Part I — Overview. *Indian Journal of Fibre & Textile Research*, 36, pp.422–428.
- Cochrane, C. et al., 2013. New design of textile light diffusers for photodynamic therapy. *Materials science & engineering. C, Materials for biological applications*, 33(3), pp.1170–5. Available at: <http://www.ncbi.nlm.nih.gov/pubmed/23827556> [Accessed September 30, 2014].
- Fauduet, H. et al., 2003. Modelling of influential parameters on a continuous evaporation process by Doehlert shells. *Journal of automated methods & management in chemistry*, 25(1), pp.21–30.
- Lee, K. & Hamid, S., 2015. Simple Response Surface Methodology: Investigation on Advance Photocatalytic Oxidation of 4-Chlorophenoxyacetic

- Acid Using UV-Active ZnO Photocatalyst. *Materials*, 8, pp.339–354. Available at: <http://www.mdpi.com/1996-1944/8/1/339/>.
- Lee, Park, K., 2009. Integration of Plastic Optical Fiber into Textile Structures.pdf.
- Mordon, S., Cochrane, C., et al., 2015. Light emitting fabric technologies for photodynamic therapy. *Photodiagnosis and Photodynamic Therapy*. Available at: <http://dx.doi.org/10.1016/j.pdpdt.2014.11.002>.
- Mordon, S., Maire, C., et al., 2015. Thérapie photodynamique en dermatologie. *Annales de Dermatologie et de Vénérologie*, 142(6–7, Supplement 2), pp.S329–S330. Available at: <http://www.sciencedirect.com/science/article/pii/S0151963815002811>.
- Wang, J., Huang, B. & Yang, B., 2013. Effect of weave structure on the side-emitting properties of polymer optical fiber jacquard fabrics. *Textile Research Journal*, 83(11), pp.1170–1180. Available at: <http://trj.sagepub.com/cgi/doi/10.1177/0040517512471751> [Accessed September 22, 2014].

